ASEAN Engineering Journal

Full Paper

TEMPERATURE DISTRIBUTION ANALYSIS IN PARALLEL PLATE TREATMENT CHAMBER FOR PULSED ELECTRIC FIELD PROCESSING: NUMERICAL STUDY

Nur Faizal Kasri, Mohamed Afendi Mohamed Piah*, Zuraimy Adzis, A. Hamzah

School of Electrical Engineering, Faculty of Engineering, Universiti Teknologi Malaysia, 81310, UTM Johor Bahru, Johor, Malaysia

Article history
Received
15 February 2021
Received in revised form
03 August 2021
Accepted
04 January 2022
Published online
31 August 2022

*Corresponding author
fendi@utm.my

Graphical abstract

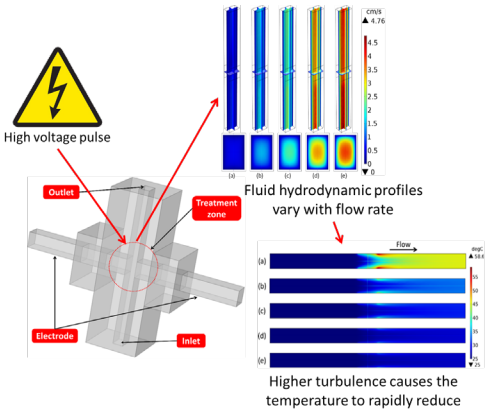

Abstract

Studies on temperature distribution in parallel plate treatment chambers are limited due to its design which is more prone to arcing, thus, neglecting its use in continuous processing. Therefore, this study discusses the temperature distribution due to Joule heating in a parallel plate treatment chamber acting in continuous mode. The numerical results predict that at a slow flow rate (i.e., 0.0234 cm3/s), the fluid flow near the chamber wall is in a static state (0 cm/s), thus, increasing its residence time and resulting in receiving more pulses. In this situation, the temperature increased dramatically from 25 °C (inlet temperature) to approximately 58 °C, i.e., 132 % increment. On the other hand, a slight increase in temperature (i.e., < 27 °C) is predicted by numerical simulation at a higher flow rate (i.e., 0.138 cm3/s) at the same location (near the chamber wall). This less rise is due to the low residence time which causes the liquid to quickly leave the treatment area, thus, getting less pulse. The temperature soar in this condition is very low which is approximately 8 % of the inlet temperature. From the results obtained, flow rate control helps to reduce the temperature rise, thus, keeping the temperature at ambient temperature or slightly above the ambient and at the same time reducing the risk of the treated media from experiencing adverse effects on its physical attributes as a result of high temperatures.

Keywords: PEF, temperature distribution, parallel plate treatment chamber, numerical simulation, flow pattern

1.0 INTRODUCTION

The nonthermal treatment technique has emerged as an alternative to the traditional method of food pasteurization. In the traditional technique, heat is used as the main agent to kill the bacteria by heating the food on the stove. In this way, it not merely kills bacteria but also adversely affects the physical properties of the food itself such as color, flavor, and nutritional content [1–3]. This drawback has pushed the scientist in the field of food technology, microbiology, and electrical engineering to synergically combine their expertise and explore the potency of the nonthermal method on food processing.

Amongst nonthermal technologies, pulsed electric field (PEF) is one of the novel methods that can significantly inactivate the food-borne pathogens and spoilage microorganisms [4, 5]. This is done by implementing short electrical pulses (nano-microseconds) to food placed between electrodes. Bacteria then experience a phenomenon called electroporation that causes its membrane to permeable. It can be achieved when the induced electric potential across the living cell membrane due to the application of an electric field, exceeding the critical value of approximately 1 V. This will result in the formation of pores in the weak areas of the membrane caused by the repulsion between charge-carrying molecules [6–10].

According to [11] and [12], the electric field distribution is determined by the treatment chamber geometric design. As for a parallel electrode configuration, it is the only known arrangement that can produce the most uniform electric field

distribution where it can enhance the rate of microbial inactivation. However, arcing is the only hurdle that made this design disregarded to be implemented in continuous processing [13]. The phenomenon of arcing occurs in the middle of the treatment zone when there is an equal amount between electric fields applied and the dielectric strength of the food. It is usually seen as a spark. This spark creates a passage that allows substantial electrical current to flow, thus, causing the food to experience a condition of dielectric breakdown [14].

The study of the treatment chamber is crucial in this area as it is not merely used to approximate the uniformity of the electric field formation but also can predict the temperature rise due to the effect of Joule heating. Since continuous processing is implemented, the study of fluid flow patterns is also important to note because it can have a huge impact on temperature distribution at each point of the fluid. However, all these are intricate to be determined experimentally which leads to the employment of computational modeling [15–18].

This paper presents a numerical simulation study of temperature rise in treatment areas that ultimately affects the conductivity of the treated media. Also, the effects of fluid flow patterns are highlighted as they are believed can be exploited in controlling liquid temperature. This study aims to analyze the temperature distribution across the parallel plate treatment chamber in continuous processing that highly depending on the fluid velocity. The order of the electrode has been set in parallel as it could obtain higher electric field intensity with lower peak voltage while also providing uniform electric field dispersion [19].

2.0 MATEMATHICAL MODELING

2.1 Geometrical Configuration

The geometrical configuration of the treatment chamber for this study was determined as a parallel plate and was built in COMSOL Multiphysics® for further assessment. The design of the chamber is illustrated in Figure 1. Regarding the treatment zone volume, it has been set according to the area of the electrode (3 mm × 3 mm) times with the gap between it (2 mm), thus, the total treatment volume is approximately 18 mm3 (3 mm × 3 mm × 2 mm) for each process.

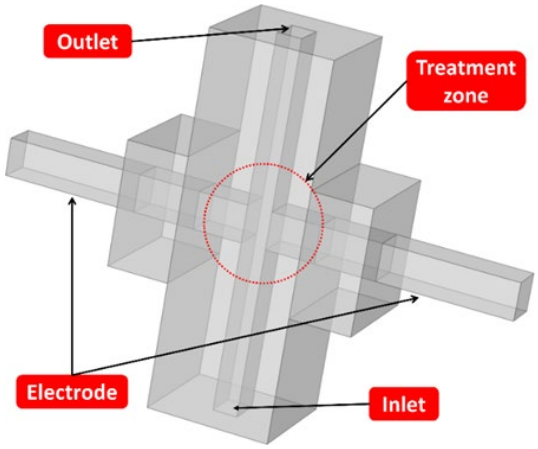

Figure 1 3D view of the parallel plate treatment chamber

2.2 Governing Equations

The finite element method (FEM) through COMSOL Multiphysics® has been used to accurately model the condition of the treatment. To integrate electric fields, flow patterns, and temperature differences, three modules have been combined: AC/DC module to complete the distribution of electric fields across the treatment gap, the Fluid Flow module to illustrate the fluid flow patterns (k-ε model applied if the flow pattern is turbulent) and the Heat Transfer module to describe the energy balance with transport by conduction and convection. All the governing equations have been adapted directly from COMSOL Multiphysics®.

2.2.1 Electric Field

The electric field dissemination across the treatment gap was estimated by solving the law of charge conservation, which for a stationary field is equal to:

$$E = -\nabla V \tag{1}$$

Where E is the amplitude of the electric field and V is the electric potential applied on the electrode. For this specific technology, E can be considered as irrotational ($\nabla \times E = 0$) as the magnetic field is ignored which allows the electric field to be expressed as a negative gradient of V.

2.2.2 Fluid Flow

The fluid flow in the treatment area is governed by the equations of continuity to describe the conservation of mass:

$$\frac{\partial \rho}{\partial t} + \nabla(\rho v) = 0 \tag{2}$$

And conservation of momentum to solve the velocity field:

$$\rho\left(\frac{\partial v}{\partial t} + v \cdot \nabla v\right) = -\nabla P + \nabla[\mu + \mu_T \nabla v] + \rho g \tag{3}$$

Where ρ is the fluid density, t is the time, v is the velocity vector, P is the pressure, μ is the dynamic viscosity, and g is the gravity acceleration constant which equals 9.81 m/s^2. On the left-hand side of Eq. 3, two terms define the rate of increase of momentum per unit of volume and the rate of momentum addition by convection per unit of volume respectively. On the other side of the same equation, there are several parameters such as pressure, viscosity, and gravity added together to represent the balancing force responsible for the fluid movement [20].

2.2.3 Heat Transfer

The governing equation for thermodynamic behavior is described by energy conservation [15], thus, the Joule heating can be stated as:

$$Q = \sigma E \cdot E = \sigma E^2 \tag{4}$$

Where Q is the heat dissipated per unit of volume, σ is the media conductivity and E is the electric field strength. To conduct

the simulation study in time-independent, a multiplication factor of time-averaged potential φ was introduced in Eq. 5. For rectangular pulses, the factor φ can be simplified as the product of pulse width τ and its frequency f.

$$\varphi = \tau \cdot f \tag{5}$$

This will result in the temperature rise in each volume of the fluid and can be assumed to be accurately captured when the fluid residential time in the treatment volume is large compared to the time interval between pulses [21].

The Q then gives rise to the increment of local temperature and heat energy transport. By solving the energy conservation equation and coupled with the equations of continuity and momentum conservation (Eq. 2 and 3), they were used to calculate the convection. Therefore, the equation for energy transport can be expressed as:

$$\rho C_p \left[\frac{\partial T}{\partial t} + v \cdot \nabla T\right] = \nabla[k + k_T \cdot \nabla T] + Q \tag{6}$$

Where k, kT, and C_P are thermal conductivity, turbulent thermal conductivity, and specific heat capacity of fluid respectively. The left-hand-side consists of two terms: (1) representing the rate of increase of internal energy per unit of volume and (2) representing the rate of addition of internal energy per unit of volume by convection. On the right-hand side, three terms added together and appear as $\nabla \cdot k\nabla T$, $\nabla \cdot k_T\nabla T$ and Q. Each one represents the addition rate of energy by conduction, the addition rate of energy due to turbulent energy dissipation, and the rate of heat generation due to Joule heating that has been multiplied with time-averaged potential factor Eq. 5 respectively.

2.3 Boundary Condition

The boundary condition for each module used needs to be defined at the foundation level to satisfy the numerical simulation requirement. The initial value for every application node should be clearly stated to avoid errors in convergence while running the simulation.

2.3.1 Electrical Conditions

The boundary condition of the electrode which in contact with the liquid flow has been defined as electric potential by setting V = 4 kV. To obtain a potential difference between two electrodes, the lower electrode was grounded by setting V = 0 on its boundary condition. The other boundaries such as the inlet, outlet, including the treatment chamber body were assumed to be electrically insulated where the current density normal to those surfaces was set to 0. For the time average potential ϕ the frequency and the pulse width have been set to 125 Hz and 1 µs respectively. It means the liquid will be suppressed by an infinite rectangular pulse (amplitude = 4 kV, pulse width = 1 µs, and frequency = 125 Hz).

2.3.2 Hydrodynamic Conditions

The inlet channel was set to fully developed flow boundary condition on the bottom part. Under a fully developed flow boundary condition, the flow rate quantity has been selected. The outlet channel was set on the top and its boundary condition was defined at 1 atmospheric pressure. The gravitational acceleration constant was also included and applied parallel to the z-axis of the geometry but in the opposite direction of liquid flow.

The automatic wall function boundary condition has been provided in the simulation software. It is a combination between the robustness of wall functions and the accuracy of low Re models to treat the extreme gradient close to the wall. It adapts the formulation to the available mesh by considering the size of the boundary layer mesh. By defining this boundary condition to the wall of the chamber, the velocity profile all the way to the wall will be accurately resolved.

2.3.3 Thermal Conditions

In heat transfer equations, the initial value boundary condition was applied to all boundaries with 25 °C including the inlet channel. The outlet channel, however, was defined with an outflow boundary condition by assuming a zero normal temperature gradient. The wall of the fluid flow area in contact with the liquid flow was assumed to be thermally insulated.

2.4 Material Properties

The liquid used was a sodium chloride (NaCl) solution. All relevant properties such as density, viscosity, thermal conductivity, and specific heat capacity are strongly dependent on temperature [21]. The correlation was made for the solution which includes various conductivity at a temperature of 15 – 80 °C and then fitted on the following equation:

$$\sigma_T = \sigma_{20}[1 + 0.024264(T - 20)] \tag{7}$$

Where σ_T is the conductivity at temperature T in °C and σ_{20} is the conductivity at 20 °C. The verification of the correlation was done experimentally using saline water with an adjusted conductivity of 0.06 S/m at 20 °C [17]. Other materials properties were provided by the COMSOL Multiphysics® database and were in the function of temperature except for the relative permittivity of water which was constant.

2.5 Numerical Simulation Procedure

The approach of two steps computational method was performed. The first step was implemented to solve the law of conservation of charge (Eq. 1) with a conjugate gradient solver and residual tolerance of 0.01. Since the formation of electric fields is independent with temperature function and highly depending on voltage and electrode arrangement, it is solved in the first step. The generated results were linked to the second step.

Next, momentum and energy equations (Eq. 3 and Eq. 6) were coupled together in an independent time study, and with the execution of segregated algorithms, the computational problems were solved. Moreover, the heat source term Q (Eq. 4) was approximated by electric field intensity produced in the first step and was multiplied by the factor φ (Eq. 5). The temperature profiles, velocity, pressure, and turbulence variables were estimated by the parallel direct solver (PARDISO). All direct solvers were specified relative to tolerance with errors estimated below 10^{-3} to obtain convergence.

3.0 RESULTS AND DISCUSSION

3.1 Electric Field Characteristic

Figure 2 illustrates the distribution of the estimated electric field within the treatment zone obtained by solving the charge conservation law (Eq. 1) for a salt solution of conductivity of 0.0673 S/m at 25 ºC. Referring to the same figure, the average volumetric electric field was approximately 20 kV/cm with an applied voltage of 4 kV and a treatment gap of 2 mm.

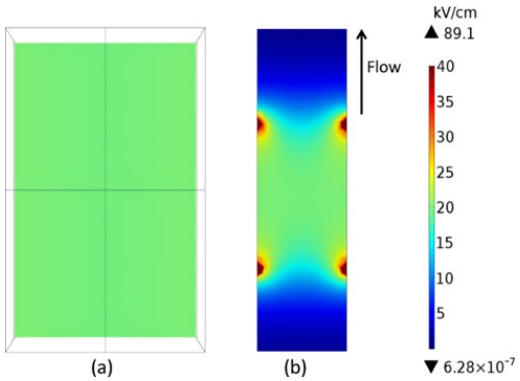

Figure 2 Predicted electric field profile for the parallel plate treatment chamber. The fluid flow starts from the bottom up. From left to right: (a) a view taken from a horizontal plane depicting a uniform electric field distribution in the treatment zone; (b) a view taken from a coronal plane showing the local peak of the electric field focusing on each edge of the electrode

According to Figure 2(a), the simulation result has shown that the parallel plate generates a uniform electric field distribution profile with an average field strength of 20 kV/cm in every corner of the treatment zone. This indicates that the fluid flow inside it (in this case NaCl solution) will have a homogeneous treatment experience. However, in Figure 2(b) it reveals the strength of the localized peak field at each edge of the electrode or in and out of the treatment zone. This condition is expected to affect the temperature rise especially in the fluid stream located far from the central axis.

3.2 Fluid Flow Characteristic

The flow rate of the fluid that flows in the treatment area was determined by the actual calibration velocity of the peristaltic pump. It begins at 20 rpm (revolution per minute) and ends at 100 rpm with an increment order of 20 rpm. Table 1 summarizes the relationship between the actual speed of the peristaltic pump and the flow rate used in the numerical simulation. The flow rate was obtained by multiplying the velocity with the area of the treatment zone.

Table 1 Velocity and flow rate relationship

Pump speed (rpm)	Velocity (cm/s)	Treatment chamber area (cm^2)	Calculated flow rate (cm^3/s)
20	0.39		0.0234
40	0.84		0.0504
60	1.23	0.06	0.0738
80	2		0.1200
100	2.3		0.1380

Fluid hydrodynamic profiles are a key attribute for characterizing flow patterns whether they flow in laminar or turbulent. Not only that, but it is also used to estimate fluid residence time when passes the treatment zone. Based on the velocity stated in Table 1, fluid flow patterns were categorized into laminar classes where the Re obtained was less than 2300 even for 100 rpm. The residence time of each rpm was estimated by taking the ratio between total treatment volume and liquid volumetric flow rate resulting in 0.77 s, 0.36 s, 0.24 s, 0.15 s, and 0.13 s for 20 rpm, 40 rpm, 60 rpm, 80 rpm, and 100 rpm respectively. Figure 3 illustrates the predicted hydrodynamic profiles for each simulated flow rate.

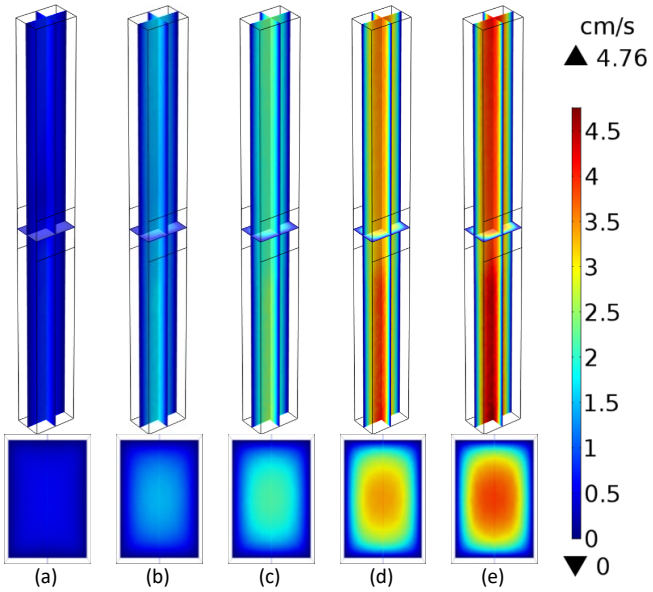

Figure 3 Predicted hydrodynamic profiles that flow in the parallel plate treatment chamber for each simulated flow rate. From left to right: (a) 20 rpm; (b) 40 rpm; (c) 60 rpm; (d) 80 rpm; (e) 100 rpm. All view was taken from perspective and horizontal plane

According to Figure 3, fluid flow velocity increases as peristaltic pump rpm increases. For a flow rate of 0.138 cm^3/s, the estimated fluid velocity was approximately 4.5 cm/s and is mostly located near the central axis, however, it slows down when it reaches the treatment chamber wall and may stop. Due to the laminar flow pattern, the fluid does not mix (acts in layers that slide over one another parallel to the wall) resulting in visible segmentation based on the fluid velocity as shown in the horizontal plane view. The main concern here is the fluid flowing near the wall as it may be static and has a velocity of 0 cm/s. This condition results in the fluid having a high residence time and receiving long exposure to electric fields compared to the fluid passing through the center. Therefore, the temperature rise in this region is expected to be high, especially in the electrode edges (Figure 2(b)) where the local peak field strength is high.

3.3 Temperature Characteristic

The escalation in temperature is due to the energy transition of Joule heating (Eq. 4) to the fluid flows passing the treatment zone. However, such increment is highly dependent on the flow rate. This is because higher velocities promote faster convective transport of thermal energy, thus, reduce the temperature rises. Figure 4 illustrates the predicted temperature distribution across

the treatment zone for 20 rpm – 100 rpm. The volumetric averaged of the electric field was predicted as shown in Figure 2 which was uniform with the intensity of 20 kV/cm. The inlet temperature and fluid conductivity were set to 25 °C and 0.067 S/m at 25 °C respectively.

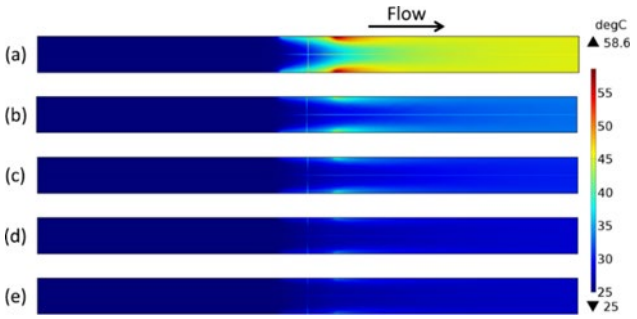

Figure 4 Predicted temperature profiles across the treatment chamber with an average electric field of 20 kV/cm, inlet temperature of 25 °C, and conductivity of 0.067 S/m at 25 °C. From top to bottom: (a) 20 rpm; (b) 40 rpm; (c) 60 rpm; (d) 80 rpm; (e) 100 rpm

According to Figure 4, the temperature rise was reduced by increasing the peristaltic pump speed. Starting with the speed of 20 rpm, the fluid temperature increased from 25 °C at the inlet to 45.8 °C on average at the outlet. The increase in temperature was recorded at almost 50 % as fluid flowed slowly causing it to be exposed to electric fields for a long time (residence time = 0.77 s), especially near the wall. This causes the fluid to receive sufficient thermal energy and thus results in a significant increase in temperature especially in the electrode corner region as illustrated in Figure 4 (a).

Figure 5 shows the relationship between average temperatures, no. of pulses, and pump speeds by plotting each parameter in one graph. As can be seen, the pattern between the average temperature and no. of pulses was akin to each other i.e., decreasing exponentially. Pump speed appears to be the main point for lowering the temperature dramatically by reducing the reception no. of pulses on the treated media. Regarding temperature alleviation, approximately 39 % of the outlet temperature (45.8 °C) was reduced to 28.1 °C when the pump speed was set to 100 rpm. This condition causes the fluid to receive only about 16 pulses, thus, makes it close to the input temperature of 25 °C at the inlet.

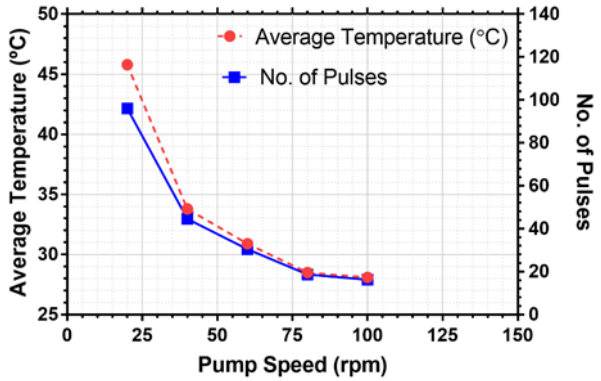

Figure 5 The predicted average temperature at the outlet and no. of pulses vs pump speed. It is seen that the pump speed can greatly reduce the temperature rise of the fluid as well as no. of pulses

To preserve the temperature between inlet and outlet, pump speed must be extended beyond 100 rpm. However, in this case, it is not possible because of the limitations of pump specifications. Higher speed means lower residence time and as consequences, fewer pulses are received by the liquid flow passing the treatment zone, thus, reduce the temperature escalation. To ensure that all liquids are treated, it must receive at least one pulse, therefore, its speed needs to be controlled properly to avoid conditions where the liquid misses the pulse.

The number of pulses plays an important role in establishing the treatment time but at the same time induces a rise in temperature. This should be considered to prevent fluids from suffering from high temperatures which can cause detrimental effects on their physical attributes. While treating liquid media is the main goal, a prevention plan must be included to avoid any significant increase in temperature as it should be maintained within the allowable range (< 70 °C).

3.4 Conductivity Characteristic

The resistance of the treatment chamber can be determined by the ratio between the treatment gap and the product of the effective electrode area and fluid conductance. Because the treatment gap and the effective electrode area are fixed parameters, the liquid conductivity is the only variable that responds to the effect of temperature rise as mentioned in 2.4. Therefore, it is important to control the degree of fluid conductance from rising sharply, otherwise, it will lead to low resistance.

According to Ohm's law, low resistance will cause the current to flow easily and this eventually drives the high current to flow through the treatment chamber. Besides, excessive current can also cause damage to the system and give rise to safety issues. This can lead to the occurrence of unwanted high current flows which poses a problem of higher energy required to achieve a certain electric field intensity [22]. Therefore, fluid conductivity must be limited to a certain level of acceptance aimed at reducing such risks. Figure 6 illustrates the predicted fluid conductivity after passing through the treatment area.

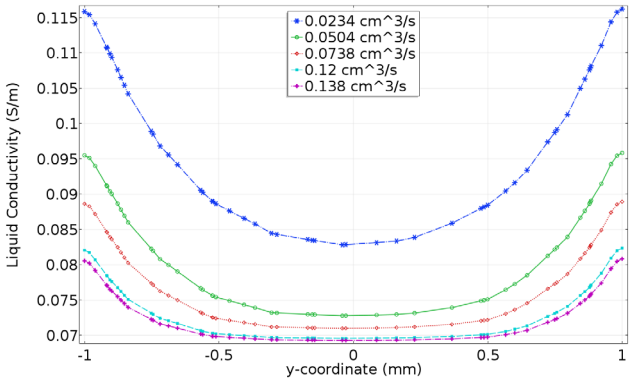

Figure 6 Predicted conductivity of NaCl solution with various flow rates. It is observed that higher flow rates reduce the temperature rise and thus decrease the conductivity. Measurement was taken parallel to the sagittal plane of the treatment chamber

In the initial stage, the conductivity of the solution is set to 0.067 S/m at 25 °C and after passing through the treatment zone it increases sharply especially in the area near the wall. The proof is, at a flow rate of 0.0234 cm^3/s, the conductivity of the liquid near the wall increases to 0.155 S/m (an escalation of almost 72 %). This indicates that in this area the temperature is high (around 58.6 °C which is an increase of around 130 %). However, when the flow rate increased to 0.138 cm^3/s, conductivity was found to be low near the wall with an increase of only 0.08 S/m or 19.4 %. This indicates that the temperature is successfully reduced due to the increase in fluid flow velocity.

In the vicinity of the central axis, the conductivity was not significantly affected. This is because the fluid velocity is higher in this region compared to the area near the wall as shown in Figure 3. This indicates that the residence time in this region is low which results in the lack of exposure to the electric field. Higher velocity also helps to promote faster convective transport of thermal energy, hence, reduce the temperature from soaring.

3.5 Energy Consumption

The method of calculating the energy dissipated as heat is done by performing volume integration on the full computational domain (treatment area) of the time-averaged Joule-heating per unit of volume from Eq. 4. The results obtained are as expected where it uses less energy compared to the traditional pasteurization method which uses heat as the main tool for microbial inactivation [23]. Table 2 shows the summary of energy dissipated as heat relative to the flow rate of the fluid and average temperature at the outlet.

Table 2 Summary of energy dissipated as heat relative to the flow rate of the fluid and average temperature

Flow rate (cm^3/s)	Energy dissipated (W)	Average Temperature (°C)
0.0234	2.0227	45.8
0.0504	1.8157	33.8
0.0738	1.7478	30.9
0.1200	1.6863	28.5
0.1380	1.6728	28.1

According to Table 2, energy dissipated as heat for the slow flow rate is higher compared to the fast flow rate, which is around 2 W. While the flow rate was set to 0.138 cm^3/s (peristaltic pump speed = 100 rpm), energy lost due to heat is approximately 1.67 W by yielding 28.1 °C of average temperature at the outlet. The reduction in energy was significant at 16.5 % and 12.4 % away from the inlet temperature. During this time, the NaCl solution receives around 16 pulses, of which two pulses less than the last second flow rate. It is expected that if the pump speed can exceed 100 rpm, the energy dissipated as heat can be decreased significantly by reducing the no. of pulses received. Note that the amplitude and the pulse width of the pulse applied were set to 4 kV and 1 µs respectively.

From the results of simulations on energy consumption, it can be concluded that PEF treatment is energy efficient compared to traditional pasteurization which using thermal. This is proven by the findings of the simulation study as tabulated in Table 2 and this result is in tandem with the findings from [22], [23], and [24]. All these researchers stated the same finding which is low energy consumption.

4.0 CONCLUSION

From the analysis presented, it is found that the parallel plate of the treatment chamber is capable of producing uniform electric field propagation throughout the treatment area. This can have a favorable effect on the homogeneous microorganism inactivation. In contrast, with the ability of the available peristaltic pumps, it can produce only laminar flow patterns. In this pattern, there are no cross-currents perpendicular to the direction of flow, nor eddies or swirls of fluids. Therefore, temperature distribution cannot be uniformly applied to each fluid point resulting in local heating. Turbulent flow is suggested to solve this issue in which a more powerful pump is needed.

Problems with significant rising temperatures can cause an unwanted current flow by increasing the conductivity of the liquid resulting in a low resistance treatment chamber. However, this can be avoided by increasing the flow rate to a certain extent until a turbulent flow pattern is obtained. In general, a parallel plate treatment chamber can be performed continuously as long as the flow rate is properly controlled, set the limit to the applied voltage, and design the appropriate treatment chamber considering the maximum allowable conductivity. Therefore, arcing problems can be avoided, and homogenous treatment can be obtained as well as enhance the inactivation rate of microorganisms.

Acknowledgement

The authors would like to thank Universiti Teknologi Malaysia (UTM), for the use of facilities and by awarding research grants: Grant UTM-TDR 46, Vot.Q.J130000.3551.07G60 and UTM-TDR 46.3, Vot.Q.J130000.3551.06G14.

References

[1] Castro, Armando J., Gustavo V. Barbosa-Cánovas, and Barry G. Swanson. 1993"Microbial inactivation of foods by pulsed electric fields." *Journal of Food Processing and Preservation* 17(1): 47-73.

[2] Barbosa-Cánovas, Gustavo V., et al. 1999.*Preservation Of Foods With Pulsed Electric Fields*. Elsevier,

[3] Mohamed, Maged EA, and Ayman H. Amer Eissa. 2012 "Pulsed electric fields for food processing technology." *Structure And Function Of Food Engineering* 11: 275-306.

[4] Gulyi, I. S., et al. 1994. "Scientific and practical principles of electrical treatment of food products and materials." Kiev: UkrINTEI (in Russian)

[5] Barsotti, L., and J. C. Cheftel. 1999"Food processing by pulsed electric fields. II. Biological aspects." *Food Reviews International* 15(2): 181-213.

[6] Zimmermann, U., et al. 1976 "Effects of external electrical fields on cell membranes." *Bioelectrochemistry And Bioenergetics* 3(1): 58-83.

[7] Benz, R., F. Beckers, and U. Zimmermann. 1979"Reversible electrical breakdown of lipid bilayer membranes: a charge-pulse relaxation study." *The Journal of membrane biology* 48(2): 181-204.

[8] Benz, R., and U. Zimmermann. 1980"Pulse-length dependence of the electrical breakdown in lipid bilayer membranes." *Biochimica et Biophysica Acta (BBA)-Biomembranes* 597(3): 637-642.

[9] Chang, Donald C., and Thomas S. Reese. 1990 "Changes in membrane structure induced by electroporation as revealed by rapid-freezing electron microscopy." *Biophysical journa*l 58(1): 1-12.

[10] Zhang, Qinghua, Gustavo V. Barbosa-Cánovas, and Barry G. Swanson. 1995"Engineering aspects of pulsed electric field pasteurization." *Journal of food engineering* 25(2): 261-281.

[11] Lindgren, Martin, et al. 2002 "Simulation of the temperature increase in pulsed electric field (PEF) continuous flow treatment chambers." *Innovative Food Science & Emerging Technologies* 3(3): 233-245.

[12] Barbosa-Cánovas, Gustavo V., and Bilge Altunakar. 2006 "Pulsed electric fields processing of foods: an overview." *Pulsed electric fields technology for the food industry*.3-26.

[13] Masood, Hassan, et al. 2018 "A comparative study on the performance of three treatment chamber designs for radio frequency electric field processing." *Computers & Chemical Engineering* 108: 206-216.

[14] Krasuchi, Z. 1968. "Breakdown of commercial liquid and liquid-solid dielectrics." High voltage technology, Alston LL (Ed), 122-128. Oxford University Press, London, UK

[15] Chen, Xiao Dong. 2006."Modeling thermal processing using computational fluid dynamics (CFD)." SUN, DW T*hermal food processing: new technologies and quality issues*. Boca Raton: CRC

[16] Schroeder, Stefanie, Roman Buckow, and Kai Knoerzer. 2009. "Numerical simulation of pulsed electric field (PEF) processing for chamber design and optimization." I*nternational Conference on CFD in the Minerads and Process Industries CSIRO,* 17th, Australia.

[17] Buckow, Roman, et al. 2010 "Simulation and evaluation of pilot-scale pulsed electric field (PEF) processing." *Journal of Food Engineering* 101(1): 67-77.

[18] Masood, Hassan, et al. 2018"A comparative study on the performance of three treatment chamber designs for radio frequency electric field processing." *Computers & Chemical Engineering* 108: 206-216.

[19] Jeyamkondan, S., D. S. Jayas, and R. A. Holley. 1999"Pulsed electric field processing of foods: a review." J*ournal Of Food Protection* 62(9): 1088-1096.

[20] Bird, R. Byron. 2002"Transport phenomena." *Appl. Mech. Rev.* 55(1): R1-R4.

[21] Gerlach, D., et al. 2008"Numerical simulations of pulsed electric fields for food preservation: a review." *Innovative Food Science & Emerging Technologies* 9(4): 408-417.

[22] Jaeger, Henry, et al. 2010"Model for the differentiation of temperature and electric field effects during thermal assisted PEF processing." *Journal of Food Engineering* 100(1): 109-118.

[23] Morales-de La Peña, M., P. Elez-Martínez, and O. Martín-Belloso. 2011 "Food preservation by pulsed electric fields: an engineering perspective." *Food Engineering Reviews* 3(2): 94-107.

[24] Ho, S. Y., G. S. Mittal, and J. D. Cross. 1997 "Effects of high field electric pulses on the activity of selected enzymes." *Journal of food engineering* 31(1): 69-84.

[25] S. Y. Ho, G. S. Mittal, and J. D. Cross, *1999,* "Effects of high field electric pulses on the activity of selected enzymes," J. Food Eng., 1997Versavel, J. 1999. Road Safety Through Video Detection. *Intelligent Transportation System, Proceedings 1999 IEEE/IEEJ/JSAI International Conference*. 753-757.